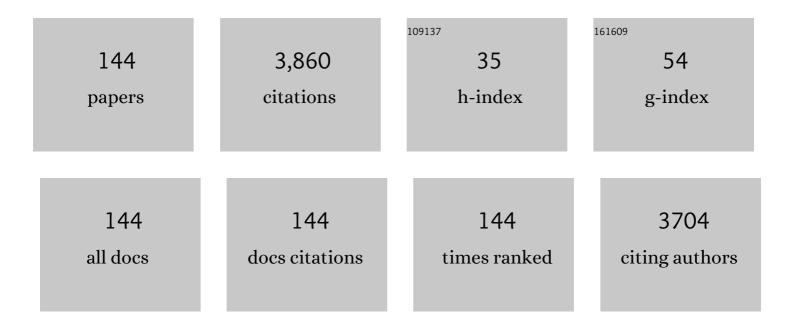
## Raul Gago

## List of Publications by Year in descending order

Source: https://exaly.com/author-pdf/9282897/publications.pdf Version: 2024-02-01



#	Article	IF	CITATIONS
1	Soft X-ray absorption study of sputtered tin oxide films. Journal of Alloys and Compounds, 2022, 902, 163768.	2.8	4
2	Correlated effects of fluorine and hydrogen in fluorinated tin oxide (FTO) transparent electrodes deposited by sputtering at room temperature. Applied Surface Science, 2021, 537, 147906.	3.1	4
3	Highly ordered silicide ripple patterns induced by medium-energy ion irradiation. Physical Review B, 2020, 102, .	1.1	6
4	In Situ Monitoring of Alkanethiol Selfâ€Assembly onto Zinc Selenide: The Role of Substrate Pretreatment and Its Implication in Bacterial Attachment. Advanced Materials Interfaces, 2020, 7, 2000848.	1.9	1
5	Morphological impact of low-energy Xe <sup>+</sup> irradiation on polycrystalline titanium targets. Journal of Physics: Conference Series, 2020, 1593, 012041.	0.3	1
6	Chemical Functionalization of the Zinc Selenide Surface and Its Impact on Lactobacillus rhamnosus GG Biofilms. ACS Applied Materials & Interfaces, 2020, 12, 14933-14945.	4.0	7
7	Anomalous Heat Transport in Nanolaminate Metal/Oxide Multilayer Coatings: Plasmon and Phonon Excitations. Coatings, 2020, 10, 260.	1.2	0
8	Soft X-ray absorption study of tantalum incorporation in titanium oxide films: Impact of flash-lamp annealing. Ceramics International, 2020, 46, 15772-15778.	2.3	2
9	Phase Selectivity in Cr and N Co-Doped TiO2 Films by Modulated Sputter Growth and Post-Deposition Flash-Lamp-Annealing. Coatings, 2019, 9, 448.	1.2	3
10	Ultraviolet to infrared downshifting in Ce and Yb co-doped aluminum oxynitride thin films. Journal Physics D: Applied Physics, 2019, 52, 285105.	1.3	0
11	Growth of nanocolumnar thin films on patterned substrates at oblique angles. Plasma Processes and Polymers, 2019, 16, 1800135.	1.6	11
12	Special issue on surfaces patterned by ion sputtering. Journal of Physics Condensed Matter, 2018, 30, 450301.	0.7	1
13	Interconnections between Electronic Structure and Optical Properties of Multilayer Nanolaminate TiAlN/Ag and Al2O3/Ag Coatings. Coatings, 2018, 8, 290.	1.2	1
14	Surface morphology of amorphous SiO <sub>2</sub> substrates bombarded with 1.0 MeV Si <sup>+</sup> ions. Journal of Physics Condensed Matter, 2018, 30, 274005.	0.7	2
15	Ultraviolet optical excitation of near infrared emission of Yb-doped crystalline aluminum oxynitride thin films. Journal of Applied Physics, 2018, 124, 033102.	1.1	2
16	Surface morphology of molybdenum silicide films upon low-energy ion beam sputtering. Journal of Physics Condensed Matter, 2018, 30, 264003.	0.7	10
17	Structural impact of chromium incorporation in as-grown and flash-lamp-annealed sputter deposited titanium oxide films. Journal of Alloys and Compounds, 2017, 729, 438-445.	2.8	7
18	Strong Room Temperature Blue Emission from Rapid Thermal Annealed Cerium-Doped Aluminum (Oxy)Nitride Thin Films. ACS Photonics, 2017, 4, 1945-1953.	3.2	12

#	Article	IF	CITATIONS
19	Features of electronic and lattice mechanisms of transboundary heat transfer in multilayer nanolaminate TiAlN/Ag coatings. Scientific Reports, 2017, 7, 17078.	1.6	3
20	The confinement of phonon propagation in TiAlN/Ag multilayer coatings with anomalously low heat conductivity. Applied Physics Letters, 2016, 108, .	1.5	4
21	Structural properties and corrosion resistance of tantalum nitride coatings produced by reactive DC magnetron sputtering. RSC Advances, 2016, 6, 89061-89072.	1.7	65
22	Electrochemical behavior of nanocrystalline Ta/TaN multilayer on 316L stainless steel: Novel bipolar plates for proton exchange membrane fuel-cells. Journal of Power Sources, 2016, 322, 1-9.	4.0	74
23	Influence of electronic structure, plasmon-phonon and plasmon-polariton excitations on anomalously low heat conductivity in TiAlN/Ag nanoscale multilayer coatings. Current Applied Physics, 2016, 16, 459-468.	1.1	9
24	Bonding structure and morphology of chromium oxide films grown by pulsed-DC reactive magnetron sputter deposition. Journal of Alloys and Compounds, 2016, 672, 529-535.	2.8	17
25	Nonuniversality due to inhomogeneous stress in semiconductor surface nanopatterning by low-energy ion-beam irradiation. Physical Review B, 2015, 91, .	1.1	44
26	Interface-Induced Plasmon Nonhomogeneity in Nanostructured Metal-Dielectric Planar Metamaterial. Journal of Nanomaterials, 2015, 2015, 1-9.	1.5	8
27	lon damage overrides structural disorder in silicon surface nanopatterning by low-energy ion beam sputtering. Europhysics Letters, 2015, 109, 48003.	0.7	13
28	Influence of metal co-deposition on silicon nanodot patterning dynamics during ion-beam sputtering. Nanotechnology, 2014, 25, 415301.	1.3	12
29	Self-organized nanopatterning of silicon surfaces by ion beam sputtering. Materials Science and Engineering Reports, 2014, 86, 1-44.	14.8	142
30	X-ray absorption near-edge structure of hexagonal ternary phases in sputter-deposited TiAlN films. Journal of Alloys and Compounds, 2013, 561, 87-94.	2.8	26
31	Atomistic model of ultra-smooth amorphous thin film growth by low-energy ion-assisted physical vapour deposition. Journal Physics D: Applied Physics, 2013, 46, 395303.	1.3	5
32	Energy dependence of the ripple wavelength for ion-beam sputtering of silicon: Experiments and theory. , 2013, , .		1
33	Self-organized surface nanopatterns on Cd(Zn)Te crystals induced by medium-energy ion beam sputtering. Journal Physics D: Applied Physics, 2013, 46, 455302.	1.3	9
34	Independence of interrupted coarsening on initial system order: ion-beam nanopatterning of amorphous versus crystalline silicon targets. Journal of Physics Condensed Matter, 2012, 24, 375302.	0.7	22
35	Nanopatterning dynamics on Si(100) during oblique 40-keV Ar <mml:math xmlns:mml="http://www.w3.org/1998/Math/MathML" display="inline"&gt;<mml:msup><mml:mrow /&gt;<mml:mo>+</mml:mo></mml:mrow </mml:msup>erosion with metal codeposition: Morphological and compositional correlation. Physical Review B. 2012. 86</mml:math 	1.1	37
36	And compositional correlation. Physical Review B, 2012, 86, . A review of monolithic and multilayer coatings within the boron–carbon–nitrogen system by ion-beam-assisted deposition. Journal of Materials Research, 2012, 27, 743-764.	1.2	16

#	Article	IF	CITATIONS
37	Hydrogen stability in hydrogenated amorphous carbon films with polymer-like and diamond-like structure. Journal of Applied Physics, 2012, 112, .	1.1	24
38	Spectroscopic evidence of NOx formation and band-gap narrowing in N-doped TiO2 films grown by pulsed magnetron sputtering. Materials Chemistry and Physics, 2012, 136, 729-736.	2.0	17
39	Phase composition and tribomechanical properties of Ti–B–C nanocomposite coatings prepared by magnetron sputtering. Journal Physics D: Applied Physics, 2012, 45, 375401.	1.3	21
40	Stress-induced solid flow drives surface nanopatterning of silicon by ion-beam irradiation. Physical Review B, 2012, 86, .	1.1	92
41	Annealing of heterogeneous phase TiO2 films: An X-ray absorption and morphological study. Chemical Physics Letters, 2011, 511, 367-371.	1.2	11
42	Spectral evidence of spinodal decomposition, phase transformation and molecular nitrogen formation in supersaturated TiAlN films upon annealing. Acta Materialia, 2011, 59, 6287-6296.	3.8	35
43	Identification of Ternary Phases in TiBC/a  Nanocomposite Thin Films: Influence on the Electrical and Optical Properties. Plasma Processes and Polymers, 2011, 8, 579-588.	1.6	10
44	Nanoscale pattern formation at surfaces under ion-beam sputtering: A perspective from continuum models. Nuclear Instruments & Methods in Physics Research B, 2011, 269, 894-900.	0.6	49
45	Optimized allylamine deposition for improved pluripotential cell culture. Vacuum, 2011, 85, 1071-1075.	1.6	4
46	Sublattice-specific ordering of ZnO layers during the heteroepitaxial growth at different temperatures. Journal of Applied Physics, 2011, 110, 113516.	1.1	9
47	Ultrasmooth growth of amorphous silicon films through ion-induced long-range surface correlations. Applied Physics Letters, 2011, 98, 011904.	1.5	12
48	Towards nanometric resolution in multilayer depth profiling: a comparative study of RBS, SIMS, XPS and GDOES. Analytical and Bioanalytical Chemistry, 2010, 396, 2725-2740.	1.9	79
49	Surface Morphology of Heterogeneous Nanocrystalline Rutile/Amorphous Anatase TiO <sub>2</sub> Films Grown by Reactive Pulsed Magnetron Sputtering. Plasma Processes and Polymers, 2010, 7, 813-823.	1.6	19
50	Plasma Process. Polym. 9â $\in$ 10/2010. Plasma Processes and Polymers, 2010, 7, .	1.6	0
51	Establishing the mechanism of thermally induced degradation of ZnO:Al electrical properties using synchrotron radiation. Applied Physics Letters, 2010, 96, 141907.	1.5	32
52	Mg doping of InGaN layers grown by PA-MBE for the fabrication of Schottky barrier photodiodes. Journal Physics D: Applied Physics, 2010, 43, 335101.	1.3	5
53	Depth-resolved analysis of spontaneous phase separation in the growth of lattice-matched AlInN. Journal Physics D: Applied Physics, 2010, 43, 055406.	1.3	33
54	Effect of Carbon Incorporation on the Microstructure of BC <sub><i>x</i></sub> N ( <i>x</i> = 0.25, 1,) Tj ETQq0 (	0 0 rgBT /0 3.2	Overlock 10 21

2010, 22, 1949-1951.

#	Article	IF	CITATIONS
55	Extended X-ray absorption fine structure (EXAFS) investigations of Ti bonding environment in sputter-deposited nanocomposite TiBC/a-C thin films. IOP Conference Series: Materials Science and Engineering, 2010, 12, 012012.	0.3	4
56	Observation and Modeling of Interrupted Pattern Coarsening: Surface Nanostructuring by Ion Erosion. Physical Review Letters, 2010, 104, 026101.	2.9	54
57	Tribological study of hydrogenated amorphous carbon films with tailored microstructure and composition produced by bias-enhanced plasma chemical vapour deposition. Diamond and Related Materials, 2010, 19, 1093-1102.	1.8	36
58	Transition from smoothing to roughening of ion-eroded GaSb surfaces. Applied Physics Letters, 2009, 94, 193103.	1.5	15
59	Breakdown of anomalous channeling with ion energy for accurate strain determination in GaN-based heterostructures. Applied Physics Letters, 2009, 95, 051921.	1.5	5
60	Influence of steering effects on strain detection in AlGaInN/GaN heterostructures by ion channelling. Journal Physics D: Applied Physics, 2009, 42, 065420.	1.3	6
61	Hydrogen quantification in hydrogenated amorphous carbon films by infrared, Raman, and x-ray absorption near edge spectroscopies. Journal of Applied Physics, 2009, 105, .	1.1	73
62	Aluminum incorporation in Ti1â^'xAlxN films studied by x-ray absorption near-edge structure. Journal of Applied Physics, 2009, 105, .	1.1	22
63	Electronic structure and conductivity of nanocomposite metal (Au, Ag, Cu, Mo)-containing amorphous carbon films. Solid State Sciences, 2009, 11, 1742-1746.	1.5	32
64	Thermal Stability and Oxidation Resistance of Nanocomposite TiC/a  Protective Coatings. Plasma Processes and Polymers, 2009, 6, S462.	1.6	12
65	Impact of Annealing on the Conductivity of Amorphous Carbon Films Incorporating Copper and Gold Nanoparticles Deposited by Pulsed Dual Cathodic Arc. Plasma Processes and Polymers, 2009, 6, S438.	1.6	9
66	Comparative depth-profiling analysis of nanometer-metal multilayers by ion-probing techniques. TrAC - Trends in Analytical Chemistry, 2009, 28, 494-505.	5.8	51
67	Self-Organized Surface Nanopatterning by Ion Beam Sputtering. , 2009, , 323-398.		46
68	Production of nanohole/nanodot patterns on Si(001) by ion beam sputtering with simultaneous metal incorporation. Journal of Physics Condensed Matter, 2009, 21, 224009.	0.7	34
69	High-resolution hydrogen profiling in AlGaN/GaN heterostructures grown by different epitaxial methods. Journal Physics D: Applied Physics, 2009, 42, 055406.	1.3	4
70	Surface nanopatterns induced by ion-beam sputtering. Journal of Physics Condensed Matter, 2009, 21, 220301.	0.7	28
71	Aluminium incorporation in AlxGa1â^'xN/GaN heterostructures: A comparative study by ion beam analysis and X-ray diffraction. Thin Solid Films, 2008, 516, 8447-8452.	0.8	12
72	Versatile vacuum chamber for <i>in situ</i> surface X-ray scattering studies. Journal of Synchrotron Radiation, 2008, 15, 414-419.	1.0	11

Raul Gago

#	Article	IF	CITATIONS
73	Study of SiN <sub>x</sub> :H <sub>y</sub> passivant layers for AlGaN/GaN high electron mobility transistors. Physica Status Solidi C: Current Topics in Solid State Physics, 2008, 5, 518-521.	0.8	1
74	Structure and properties of silver-containing a-C(H) films deposited by plasma immersion ion implantation. Surface and Coatings Technology, 2008, 202, 3675-3682.	2.2	87
75	Smart modification of magnetron sputtered TiN surfaces for stimulated differentiation. Surface and Coatings Technology, 2008, 203, 905-908.	2.2	3
76	X-ray Spectroscopic and Magnetic Investigation of C:Ni Nanocomposite Films Grown by Ion Beam Cosputtering. Journal of Physical Chemistry C, 2008, 112, 12628-12637.	1.5	23
77	Tuning the surface morphology in self-organized ion beam nanopatterning of Si(001) via metal incorporation: from holes to dots. Nanotechnology, 2008, 19, 355306.	1.3	63
78	Rutherford backscattering spectrometry characterization of nanoporous chalcogenide thin films grown at oblique angles. Journal of Analytical Atomic Spectrometry, 2008, 23, 981.	1.6	5
79	Boron carbides formed by coevaporation of B and C atoms: Vapor reactivity, <mmi:math xmlns:mml="http://www.w3.org/1998/Math/MathML" display="inline"&gt;<mmi:mrow><mmi:msub><mmi:mi mathvariant="normal"&gt;B<mmi:mi>x</mmi:mi></mmi:mi </mmi:msub><mmi:msub><mmi:mi mathvariant="normal"&gt;C<mmi:mi>x1<mmi:mo>â^`</mmi:mo><mmi:mi>x<td><b>1.1</b> ml:mi&gt;<td>42 nml:mrow&gt;<!--</td--></td></td></mmi:mi></mmi:mi></mmi:mi </mmi:msub></mmi:mrow></mmi:math 	<b>1.1</b> ml:mi> <td>42 nml:mrow&gt;<!--</td--></td>	42 nml:mrow> </td
80	Characterization of biofunctional thin films deposited by activated vapor silanization. Journal of Materials Research, 2008, 23, 1931-1939.	1.2	13
81	Early stage of ripple formation on Ge(001) surfaces under near-normal ion beam sputtering. Nanotechnology, 2008, 19, 035304.	1.3	35
82	Direct spectroscopic evidence of self-formed C60 inclusions in fullerenelike hydrogenated carbon films. Applied Physics Letters, 2008, 92, .	1.5	34
83	Photoluminescence enhancement in quaternary III-nitrides alloys grown by molecular beam epitaxy with increasing Al content. Journal of Applied Physics, 2008, 103, 046104.	1.1	13
84	Effect of the growth temperature and the AlN mole fraction on In incorporation and properties of quaternary III-nitride layers grown by molecular beam epitaxy. Journal of Applied Physics, 2008, 104, 083510.	1.1	16
85	Detection of intrinsic stress in cubic boron nitride films by x-ray absorption near-edge structure: Stress relaxation mechanisms by simultaneous ion implantation during growth. Physical Review B, 2007, 76, .	1.1	11
86	<i>In situ</i> x-ray scattering study of self-organized nanodot pattern formation on GaSb(001) by ion beam sputtering. Applied Physics Letters, 2007, 91, .	1.5	29
87	The effect of nitrogen incorporation on the bonding structure of hydrogenated carbon nitride films. Journal of Applied Physics, 2007, 101, 063515.	1.1	19
88	Interplay between Morphology and Surface Transport in Nanopatterns Produced by Ion-Beam Sputtering. Materials Research Society Symposia Proceedings, 2007, 1059, 1.	0.1	2
89	Bonding structure of BCN nanopowders prepared by ball milling. Diamond and Related Materials, 2007, 16, 1450-1454.	1.8	27
90	Calibration of nitrogen content for GDOES depth profiling of complex nitride coatings. Journal of Analytical Atomic Spectrometry, 2007, 22, 1512.	1.6	15

#	Article	IF	CITATIONS
91	Hybrid titania–aminosilane platforms evaluated with human mesenchymal stem cells. Journal of Biomedical Materials Research - Part B Applied Biomaterials, 2007, 83B, 232-239.	1.6	7
92	Microanalysis of Ar and He bombarded biomedical polymer films. Nuclear Instruments & Methods in Physics Research B, 2007, 257, 496-500.	0.6	4
93	Universal non-equilibrium phenomena at submicrometric surfaces and interfaces. European Physical Journal: Special Topics, 2007, 146, 427-441.	1.2	28
94	Temperature influence on the production of nanodot patterns by ion beam sputtering of Si(001). Physical Review B, 2006, 73, .	1.1	64
95	Order enhancement and coarsening of self-organized silicon nanodot patterns induced by ion-beam sputtering. Applied Physics Letters, 2006, 89, 233101.	1.5	53
96	Sixfold ring clustering insp2-dominated carbon and carbon nitride thin films: A Raman spectroscopy study. Physical Review B, 2006, 73, .	1.1	70
97	Nanometric resolution in glow discharge optical emission spectroscopy and Rutherford backscattering spectrometry depth profiling of metal (Cr, Al) nitride multilayers. Spectrochimica Acta, Part B: Atomic Spectroscopy, 2006, 61, 545-553.	1.5	15
98	Structure of MgO/V/MgO(001) thin films studied by the combination of X-ray photoemission and ion beam analysis techniques. Surface Science, 2006, 600, 497-506.	0.8	8
99	Optical and compositional analysis of functional SiOxCy:H coatings on polymers. Thin Solid Films, 2006, 515, 2493-2496.	0.8	23
100	Hemocompatibility of low-friction boron–carbon–nitrogen containing coatings. Journal of Biomedical Materials Research - Part B Applied Biomaterials, 2006, 77B, 179-187.	1.6	24
101	Thin Film Growth by Ion-Beam-Assisted Deposition Techniques. , 2006, , 345-382.		6
102	Synthesis of carbon nitride thin films by low-energy ion beam assisted evaporation: on the mechanisms for fullerene-like microstructure formation. Thin Solid Films, 2005, 483, 89-94.	0.8	15
103	Molding and Replication of Ceramic Surfaces with Nanoscale Resolution. Small, 2005, 1, 300-309.	5.2	27
104	Fullerenelike arrangements in carbon nitride thin films grown by direct ion beam sputtering. Applied Physics Letters, 2005, 87, 071901.	1.5	23
105	Nitrogen incorporation in carbon nitride films produced by direct and dual ion-beam sputtering. Journal of Applied Physics, 2005, 98, 074907.	1.1	6
106	Correlation between bonding structure and microstructure in fullerenelike carbon nitride thin films. Physical Review B, 2005, 71, .	1.1	40
107	Self-Organized Ordering of Nanostructures Produced by Ion-Beam Sputtering. Physical Review Letters, 2005, 94, 016102.	2.9	212
108	Evolution ofsp2networks with substrate temperature in amorphous carbon films: Experiment and theory. Physical Review B, 2005, 72, .	1.1	61

#	Article	IF	CITATIONS
109	Surface nanopatterning of metal thin films by physical vapour deposition onto surface-modified silicon nanodots. Nanotechnology, 2004, 15, S197-S200.	1.3	24
110	Structural and chemical characterization of functional SiO[sub x]C[sub y]:H coatings for polymeric lenses. Journal of Vacuum Science & Technology an Official Journal of the American Vacuum Society B, Microelectronics Processing and Phenomena, 2004, 22, 2402.	1.6	2
111	Spectroscopic ellipsometry investigation of amorphous carbon films with different sp3 content: relation with protein adsorption. Thin Solid Films, 2004, 455-456, 530-534.	0.8	37
112	Heavy-ion ERDA and spectroscopic ellipsometry characterization of a SiOC:H layered structure as functional coating on polymeric lenses. Nuclear Instruments & Methods in Physics Research B, 2004, 219-220, 908-913.	0.6	11
113	Stress measurement and stress relaxation during magnetron sputter deposition of cubic boron nitride thin films. Thin Solid Films, 2004, 447-448, 131-135.	0.8	16
114	Direct Nanopatterning of Metal Surfaces Using Self-Assembled Molecular Films. Advanced Materials, 2004, 16, 405-409.	11.1	42
115	In-depth optical and structural study of silver-based low-emissivity multilayer coatings for energy-saving applications. Journal Physics D: Applied Physics, 2004, 37, 1554-1557.	1.3	29
116	X-ray diffraction study of stress relaxation in cubic boron nitride films grown with simultaneous medium-energy ion bombardment. Applied Physics Letters, 2004, 85, 5905-5907.	1.5	13
117	Tribological properties of ternary BCN films with controlled composition and bonding structure. Diamond and Related Materials, 2004, 13, 1532-1537.	1.8	39
118	Efecto del argon en pelÃculas CN <sub>x</sub> H <sub>y</sub> depositadas mediante ECR-CVD. Boletin De La Sociedad Espanola De Ceramica Y Vidrio, 2004, 43, 491-493.	0.9	0
119	Development of interference filters based on multilayer porous silicon structures. Materials Science and Engineering C, 2003, 23, 1043-1046.	3.8	17
120	Fine structure at the X-ray absorption $\tilde{I} \in *$ and $\tilde{I} f^*$ bands of amorphous carbon. Diamond and Related Materials, 2003, 12, 110-115.	1.8	27
121	Hydrogen incorporation in CNx films deposited by ECR chemical vapor deposition. Diamond and Related Materials, 2003, 12, 632-635.	1.8	4
122	Diagnostics of a N2/Ar direct current magnetron discharge for reactive sputter deposition of fullerene-like carbon nitride thin films. Journal of Applied Physics, 2003, 94, 7059-7066.	1.1	49
123	Characterization of the unoccupied and partially occupied states of TTF-TCNQ by XANES and first-principles calculations. Physical Review B, 2003, 68, .	1.1	54
124	Direct molding of nanopatterned polymeric films: Resolution and errors. Applied Physics Letters, 2003, 82, 457-459.	1.5	13
125	Damage effects from medium-energy ion bombardment during the growth of cubic-boron nitride films. Journal of Vacuum Science and Technology A: Vacuum, Surfaces and Films, 2003, 21, 1739-1744.	0.9	3
126	Transition from amorphous boron carbide to hexagonal boron carbon nitride thin films induced by nitrogen ion assistance. Journal of Applied Physics, 2002, 92, 5177-5182.	1.1	43

#	Article	IF	CITATIONS
127	Nanopatterning of silicon surfaces by low-energy ion-beam sputtering: dependence on the angle of ion incidence. Nanotechnology, 2002, 13, 304-308.	1.3	61
128	X-Ray absorption study of the bonding structure of BCN compounds enriched in carbon by CH4 ion assistance. Diamond and Related Materials, 2002, 11, 1295-1299.	1.8	9
129	On the bonding structure of hydrogenated carbon nitrides grown by electron cyclotron resonance chemical vapour deposition: towards the synthesis of non-graphitic carbon nitrides. Diamond and Related Materials, 2002, 11, 1161-1165.	1.8	14
130	Thin Films of Molecular Metals TTF-TCNQ. Journal of Solid State Chemistry, 2002, 168, 384-389.	1.4	33
131	Deposition of TiN/AIN bilayers on a rotating substrate by reactive sputtering. Surface and Coatings Technology, 2002, 157, 26-33.	2.2	32
132	Growth and characterisation of boron–carbon–nitrogen coatings obtained by ion beam assisted evaporation. Vacuum, 2002, 64, 199-204.	1.6	36
133	Identification of ternary boron–carbon–nitrogen hexagonal phases by x-ray absorption spectroscopy. Applied Physics Letters, 2001, 78, 3430-3432.	1.5	50
134	Detecting with X-ray absorption spectroscopy the modifications of the bonding structure of graphitic carbon by amorphisation, hydrogenation and nitrogenation. Surface Science, 2001, 482-485, 530-536.	0.8	42
135	X-Ray absorption studies of cubic boron–carbon–nitrogen films grown by ion beam assisted evaporation. Diamond and Related Materials, 2001, 10, 1165-1169.	1.8	40
136	X-Ray absorption studies of bonding environments in graphitic carbon nitride. Diamond and Related Materials, 2001, 10, 1170-1174.	1.8	30
137	Hardening Mechanisms in Graphitic Carbon Nitride Films Grown with N2/Ar Ion Assistance. Chemistry of Materials, 2001, 13, 129-135.	3.2	35
138	Choice of boron–carbon–nitrogen coating material for electron emission based on photoelectric yield measurements during x-ray absorption studies. Journal of Vacuum Science & Technology an Official Journal of the American Vacuum Society B, Microelectronics Processing and Phenomena, 2001, 19, 1358.	1.6	7
139	Production of ordered silicon nanocrystals by low-energy ion sputtering. Applied Physics Letters, 2001, 78, 3316-3318.	1.5	226
140	Boron–carbon–nitrogen compounds grown by ion beam assisted evaporation. Thin Solid Films, 2000, 373, 277-281.	0.8	28
141	Spectroscopy of π bonding in hard graphitic carbon nitride films: Superstructure of basal planes and hardening mechanisms. Physical Review B, 2000, 62, 4261-4264.	1.1	68
142	Bonding and hardness in nonhydrogenated carbon films with moderate sp3 content. Journal of Applied Physics, 2000, 87, 8174-8180.	1.1	57
143	Effect of the substrate temperature on the deposition of hydrogenated amorphous carbon by PACVD at 35 kHz. Thin Solid Films, 1999, 338, 88-92.	0.8	32
144	Influence of ion current on the growth of carbon films by ion-beam-assisted deposition. Diamond and Related Materials, 1999, 8, 1944-1950.	1.8	5